Cubic Rashba Spin-Orbit Interaction of a Two-Dimensional Hole Gas in a Strained-Ge/SiGe Quantum Well

Rai Moriya,[1,*] Kentarou Sawano,[2] Yusuke Hoshi,[1,2,‡] Satoru Masubuchi,[1,3] Yasuhiro Shiraki,[2] Andreas Wild,[4,5] Christian Neumann,[5] Gerhard Abstreiter,[4,6] Dominique Bougeard,[5] Takaaki Koga,[7] and Tomoki Machida[1,3,†]

[1]*Institute of Industrial Science, University of Tokyo, 4-6-1 Komaba, Meguro-ku, Tokyo 153-8505, Japan*
[2]*Advanced Research Laboratories, Tokyo City University, 8-15-1 Todoroki, Setagaya-ku, Tokyo 158-0082, Japan*
[3]*Institute for Nano Quantum Information Electronics, University of Tokyo, 4-6-1 Komaba, Meguro-ku, Tokyo 153-8505, Japan*
[4]*Walter Schottky Institut and Physics Department, Technische Universität München, Am Coulombwall 4, 85748 Garching, Germany*
[5]*Institut für Experimentelle und Angewandte Physik, Universität Regensburg, Universitätsstraße 31, 93040 Regensburg, Germany*
[6]*Institute for Advanced Study, Technische Universität München, Lichtenbergstraße 2a, 85748 Garching, Germany*
[7]*Division of Electronics for Informatics, Graduate School of Information Science and Technology,
Hokkaido University, Hokkaido 060-0814, Japan*

The spin-orbit interaction (SOI) of a two-dimensional hole gas in the inversion symmetric semiconductor Ge is studied in a strained-Ge/SiGe quantum well structure. We observe weak antilocalization (WAL) in the magnetoconductivity measurement, revealing that the WAL feature can be fully described by the k-cubic Rashba SOI theory. Furthermore, we demonstrate electric field control of the Rashba SOI. Our findings reveal that the heavy hole (HH) in strained Ge is a purely cubic Rashba system, which is consistent with the spin angular momentum $m_j = \pm 3/2$ nature of the HH wave function.

The spin-orbit interaction (SOI) in a two-dimensional system is a subject of considerable interest because the SOI induces spin splitting at a zero magnetic field, which is important in both fundamental research and electronic device applications [1]. Recent developments of SOI-induced phenomena in the solid state demonstrate many possibilities utilizing spin current and the emergence of new physics such as the spin interferometer [2,3], persistent spin helix [4,5], spin Hall effect [6–8], and quantum spin Hall effect [9,10]. Up to now, there have been two well-known SOIs existing in solids: the Dresselhaus SOI [11] due to bulk inversion asymmetry (BIA) in the crystal structure and the Rashba SOI [12,13] due to spatial inversion asymmetry (SIA).

In low-dimensional systems, the Rashba SOI becomes more important because it is stronger at the heterointerface and can be controlled by an external electric field. Many of the pioneering studies on the SOI-induced phenomena mentioned above were performed in two-dimensional electron systems, where the Rashba SOI is described by the k-linear Rashba term. In the Hamiltonian, the k-linear Rashba term can be written as $H_{R1} = \alpha_1 E_z i(k_- \sigma_+ - k_+ \sigma_-)$, where $\sigma_\pm = 1/2(\sigma_x \pm i\sigma_y)$ denote combinations of Pauli spin matrices, $k_\pm = k_x \pm ik_y$, and k_x, k_y are the components of the in-plane wave vector $\mathbf{k}_\parallel$. The effective magnetic field $\Omega_1(\mathbf{k}_\parallel)$ acting on the transport carrier due to the k-linear Rashba term is illustrated in Fig. 1(a).

Recently, a higher-order contribution of the Rashba SOI, the so-called k^3 (k-cubic) Rashba SOI, has received more attention [14,15]. The Hamiltonian for the k-cubic Rashba SOI is expressed as $H_{R3} = \alpha_3 E_z i(k_-^3 \sigma_+ - k_+^3 \sigma_-)$ [16],

and the effective magnetic field $\Omega_3(\mathbf{k}_\parallel)$ in k space is illustrated in Fig. 1(b) [15]. There is a significant difference in the effective field symmetry between the k-linear and the k-cubic Rashba SOI with one and three rotations in k space, respectively. The k^3 symmetry of the SOI is an interesting subject because it influences all of the SOI-induced phenomena as opposed to the k-linear Rashba term. For example, in case of the spin Hall effect, the k-cubic Rashba term is predicted to give rise to a larger spin Hall conductivity [17–19].
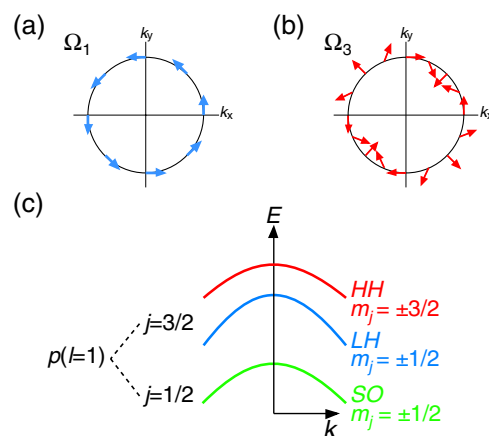

FIG. 1 (color online). (a),(b) The effective magnetic field direction with respect to the in-plane wave vector k for (a) the linear-Rashba term, Ω_1 and (b) the cubic-Rashba term, Ω_3. (c) Schematic illustration of the valence band structure for strained Ge. The HH, LH, and SO bands are indicated.

Recently, the cubic-Rashba SOI has been reported in a two-dimensional hole gas (2DHG) in inversion asymmetric semiconductors InGaAs and GaAs [20,21], and a two-dimensional electron gas formed at a surface of the inversion symmetric oxide SrTiO$_3$ [15]. However in the former case, the InGaAs and GaAs possess both BIA and SIA; thus, they are always influenced by both Dresselhaus and Rashba SOI contributions [22]. Because the Dresselhaus SOI also has k-cubic dependence, the cubic-Rashba SOI is difficult to observe independently. In the latter case, the complex electric structure of SrTiO$_3$ makes it difficult to compare with the existing Rashba theory and theoretical development on the spin orbit interaction in the perovskite oxide is still in progress. Consequently, material systems with a simple band structure and pure cubic-Rashba SOI are in high demand. Here, we propose a purely cubic-Rashba SOI system: the single element semiconductor Ge. Because Ge does not have BIA, the Dresselhaus SOI is essentially absent. Thus, the SOI in Ge is described only with the Rashba term.

The valence band structure of strained Ge around the Γ point is schematically illustrated in Fig. 1(c). The valence band hole has a p-orbital wave function with orbital angular momentum $l = 1$; therefore, it has total angular momentum $j = 3/2$ and $j = 1/2$. The $j = 3/2$ and $j = 1/2$ hole states are separated from each other due to the atomic SOI. The separated $j = 1/2$ state is called the split-off (SO) state as indicated in Fig. 1(c). The $j = 3/2$ state further splits into the $m_j = \pm3/2$ heavy hole (HH) and $m_j = \pm1/2$ light hole (LH) states. Among the hole states, the wave function described by $m_j = \pm1/2$ possesses a k-linear Rashba SOI. The k-linear Rashba SOI is also dominant in most studied conduction band electron cases since the conduction band is fully described by the $m_j = \pm1/2$ wave function. On the other hand, for $m_j = \pm3/2$, the Rashba SOI exhibits k-cubic dependence. Further, in the strained-Ge/SiGe quantum well (QW) structure, owing to compressive strain in the Ge well, the degeneracy of the HH and LH bands at $k = 0$ can be lifted. The separation between the HH and LH bands can be as large as ~100 meV with increasing amounts of strain. Thus, the top of the valence band can be tuned to the HH state. Recent advances in Ge and SiGe epitaxial growth technology revealed that it is possible to fabricate a high crystal quality strained-Ge/SiGe QW on Si substrates [23,24]. Thus, strained Ge/SiGe provides a good platform to study the cubic-Rashba SOI in simple single element semiconductors and will offer an interesting comparison with existing SOI theory.

In this Letter, we experimentally reveal cubic-Rashba SOI in a 2DHG in a strained-Ge/SiGe QW. Comparing the weak localization (WL) and weak antilocalization (WAL) measurements with the analysis of the linear- and cubic-Rashba SOI terms, we found that spin transport in the 2DHG can be fully explained by the cubic-Rashba SOI. The SOI magnitude can be controlled with the gate voltage.

These findings are all consistent with the $m_j = \pm3/2$ characteristics of the HH band in a strained-Ge QW, which obeys the cubic-Rashba Hamiltonian.

A strained-Ge/SiGe single QW is grown by using solid source molecular beam epitaxy. First, a fully relaxed Si$_{0.5}$Ge$_{0.5}$ buffer layer is grown on a Si(001) substrate. On top of this layer, the following QW structure is grown: 10 p-Si$_{0.5}$Ge$_{0.5}$/10 Si$_{0.5}$Ge$_{0.5}$/20 Ge/30 Si$_{0.5}$Ge$_{0.5}$/3 Si (units in nanometers). Due to the lattice mismatch (~2.1%) between the Ge and Si$_{0.5}$Ge$_{0.5}$ layers, the Ge QW layer is compressively strained. After patterning the wafer in the Hall bar structure, an Al$_2$O$_3$ dielectric layer with a 75-nm thickness is deposited using atomic layer deposition, and then a Pd/Au gate electrode is deposited. The application of the gate voltage enables us to tune the hole density of the 2DHG in the QW. The magnetotransport is measured in a variable temperature cryostat at the temperature range of 1.6–10 K. A magnetic field is applied perpendicular to the sample plane using a superconducting magnet.

First, the change in the sheet resistance R_{sheet} and hole concentration n_{hole} at various back gate voltages V_G is shown in Fig. 2(a). When V_G is decreased from +1.2 to −0.4 V, R_{sheet} (n_{hole}) monotonically decreases (increases). This change accompanies the variation of hole mobility
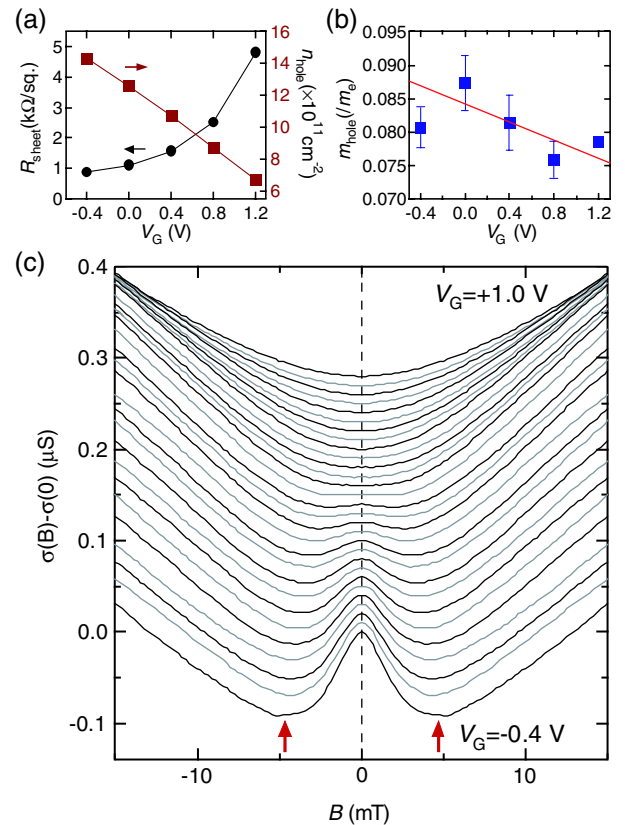

FIG. 2 (color online). (a),(b) The V_G dependence of (a) sheet resistance R_{sheet} and hole concentration n_{hole} and (b) the hole effective mass m_{hole}. (c) The change of magnetoconductivity $\Delta\sigma(B)$ measured at 1.6 K at various V_G.

from 2000 to 5200 cm^2/V s. The change in the hole effective mass m_{hole} with respect to V_G is shown in Fig. 2(b). The effective mass of the holes is determined from the temperature dependence of the Shubnikov–de Haas oscillation. The effective mass increases with the hole concentration and this is due to the nonparabolicity of the valence band [25,26].

Next, we show the change of magnetoconductivity $\Delta\sigma(B) = \sigma(B) - \sigma(0)$ measured at various V_G in Fig. 2(c). Under a gate sweep of $V_G = +1.0$ to -0.4 V, $\Delta\sigma(B)$ is significantly modulated. In the high-field region, the conductivity monotonically increases with the external magnetic field, which we attribute to the WL. Together with the WL feature, in the high hole density region ($V_G < +0.2$ V) a conductance peak appears when the magnetic field is near zero. This conductance peak is due to the WAL. The cross-over points of $\Delta\sigma(B)$, which are indicated by arrows in Fig. 2(c), shift position from low magnetic field to high magnetic field with decreasing V_G. The cross-over points are roughly proportional to the magnetic field for the SOI, B_{SO}; a larger B_{SO} produces a larger cross-over point field. Thus, our results suggest that the SOI can be tuned with the gate voltage.

Observed WL and WAL data have been analyzed by using the Iordanskii–Lyanda-Geller–Pikus (ILP) theory for magnetoconductivity, which took into account both the linear- and cubic-Rashba SOI [15,20,27]. The general formula of the ILP theory is provided in the Supplemental Material [28]. We limited our fitting to within the diffusive transport regime where the magnetic field B is within the range $B < B_{tr} = \hbar/2el_m^2$, where B_{tr} denotes the transport field characterizing the elastic scattering time of the hole, $\hbar$ is Planck's constant, e is the electron charge, and l_m is the mean free path of the hole. In the ILP theory, we only consider the Rashba SOI since there is no structural inversion asymmetry in Ge. Both k-linear Ω_1 and k-cubic Ω_3 effective magnetic fields in frequency units are incorporated [15]. Under these conditions, the fitting parameters to analyze experimental data are the characteristic magnetic fields for the phase coherence $B_\phi = \hbar/4eD\tau_\phi$, for the k-linear spin-orbit coupling $B_{SO1} = (\hbar/4eD)2|\Omega_1|^2\tau_{tr}$, and for the k-cubic spin-orbit coupling $B_{SO3} = (\hbar/4eD)2|\Omega_3|^2\tau_{tr}$, where D denotes the diffusion constant, τ_ϕ the phase coherent time of the carrier, and τ_{tr} the elastic scattering time. By setting either $B_{SO3} = 0$ or $B_{SO1} = 0$ in the ILP model, formulas with only the k-linear term or the k-cubic term are obtained [28]. In Fig. 3, we present the experimental data (open circles) and fitting results with only the k-linear term (blue dashed line) or only the k-cubic term (red solid line). We found that fitting with only the cubic-Rashba term revealed good agreement with the experimental results regardless of the V_G value, whereas the linear-Rashba term is insufficient for explaining the larger field region of the WAL data. The low magnetic field region can be fitted with both the linear- and cubic- models because this region is
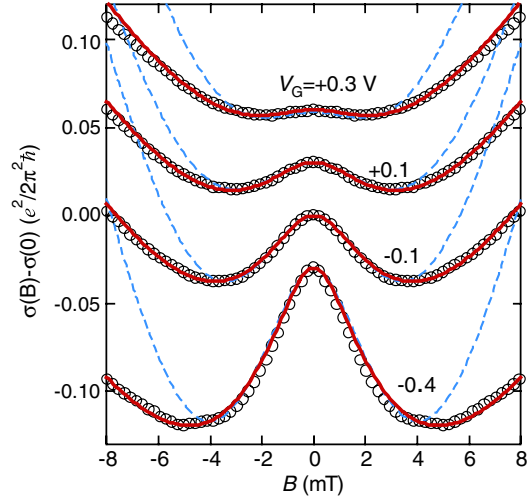

FIG. 3 (color online). The V_G dependence of the change of magnetoconductivity $\Delta\sigma(B)$ shown with the fitting results from the ILP model. Black open circles indicate experimental data, and the red solid line and blue dashed lines show calculations using the ILP model for the cubic- and linear-Rashba terms, respectively.

determined by the B_ϕ term rather than B_{SO}. However, we observed significantly different behavior between the linear- and cubic-Rashba terms in the larger magnetic field region. The cubic-Rashba model explains the experimental data more precisely; thus, we believe the cubic-Rashba model is relevant for the HH band in Ge.

Figure 4(a) shows B_{SO3} and B_ϕ obtained by fitting with the cubic-Rashba model. Both B_{SO3} and B_ϕ systematically change with V_G. When $B_{SO3} > B_\phi$, WAL is observed, and WL is observed when $B_{SO3} < B_\phi$. The change of B_{SO3} provides direct evidence of the electric field control of the cubic-Rashba SOI. Note that the change of B_ϕ with respect to V_G is due to the change of the hole mobility, and this gives rise to a longer phase coherence time τ_ϕ with increasing hole concentration. If k-dependent spin splitting due to the SOI exists, the spin relaxation is described by the Dyakonov-Perel mechanism with $\tau_{SO} \propto 1/\Delta^2\tau_{tr}$ [29], where Δ is the spin splitting energy and τ_{SO} denotes the spin relaxation time. On the other hand, if spin-flip scattering is the dominant spin relaxation mechanism, the Elliot-Yafet mechanism with $\tau_{SO} \propto \tau_{tr}/(\Delta g)^2$ (Δg is the shift of the electron g factor from that of free electrons) is relevant for describing our results. Therefore, the comparison between τ_{SO} and τ_{tr} provides additional evidence for the Rashba-type SOI. The τ_{SO} and τ_{tr} terms can be calculated using the relations $B_{SO3} = \hbar/4eD\tau_{SO}$, $D = v_F^2\tau_{tr}/2$, $v_F = \hbar k_F/m_{hole}$, and $k_F = \sqrt{2\pi n_{hole}}$, where v_F is the Fermi velocity and k_F is the Fermi wave vector. We plotted τ_{SO} and τ_{tr} with respect to the hole concentration as shown in Fig. 4(b). We found that τ_{tr} increases with increasing carrier concentration, whereas τ_{SO} decreases. This is consistent with the Dyakonov-Perel spin relaxation mechanism. Therefore, it provides further
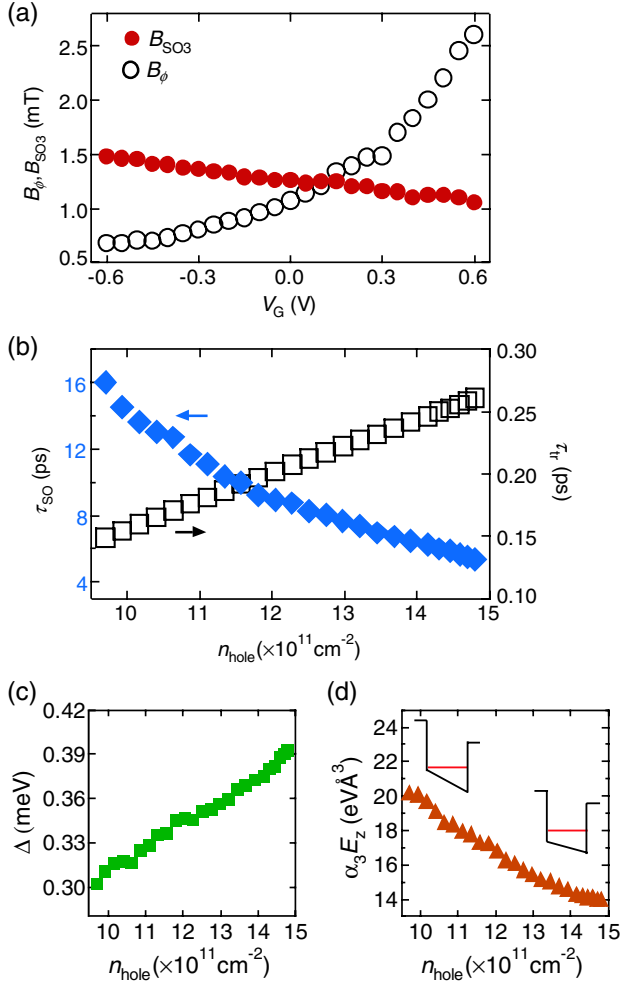
FIG. 4 (color online).   (a) The V_G dependence of the characteristic magnetic fields for the k-cubic spin-orbit coupling B_{SO3} and the phase coherence B_ϕ. (b) Hole concentration dependence of the spin relaxation time τ_{SO} and momentum scattering time τ_{tr}. (c) Spin-splitting energy Δ versus the hole concentration. (d) The change of Rashba spin-orbit coefficient $\alpha_3 E_z$ with respect to the hole concentration.

evidence that the Rashba SOI is a dominant spin-orbit contribution in the 2DHG.

The agreement between the experimental data and the k-cubic-term-only condition of the ILP theory reveals the existence of the purely cubic-Rashba SOI in the 2DHG. We now evaluate the spin splitting energy from the relationship $\Delta = \hbar|\Omega_3|$. The change of Δ with respect to hole concentration is shown in Fig. 4(c). We obtained a Δ of 0.3–0.4 meV; we find larger spin splitting with increasing hole concentration. This spin splitting provides direct experimental evidence of the cubic-Rashba SOI induced splitting in strained Ge. To analyze the splitting in more detail, we calculated the coefficient $\alpha_3 E_z$ for the cubic-Rashba SOI using the relation $\Delta = \hbar|\Omega_3| = \alpha_3 E_z k^3$, as shown in Fig. 4(d). The coefficient $\alpha_3 E_z$ decreases with increasing hole concentration. We believe that this is due to

the change of the gate-induced electric field E_z in the QW rather than a change of α_3.

Here, the Rashba coefficient α_3 for the first HH subband is expressed as follows:

$$\alpha_3 = \frac{-3e\hbar^4\gamma_3^2}{2m_0^2\left(E_{HH} - E_{LH}\right)^2}, \tag{1}$$

where γ_3 denotes the Luttinger parameter, and E_{HH} and E_{LH} are the energies of the lowest HH and LH subbands, respectively. Equation (1) is derived from the Luttinger Hamiltonian using the partitioning method presented by Ohkawa and Uemura [13]. Equation (1) suggests that α_3 is inversely proportional to the square of the separation between the HH and LH energy. A qualitatively similar expression to Eq. (1) is also reported by other groups [14,20]. In a single heterostructure, the HH-LH separation changes with the external electric field, thus demonstrating gate control of α_3 [30]. However, in the QW, the change in the HH and LH separation with external electric field should be small. Furthermore, because the HH-LH separation in the Ge/Si$_{0.5}$Ge$_{0.5}$ QW is initially large due to strain, the gate-induced change of the HH-LH separation is 1 order smaller than its total HH-LH separation energy; therefore, we think that α_3 is almost constant over the studied hole concentration range. For these reasons, we believe that the results shown in Fig. 4(d) reflect the change of the effective electric field in the QW under the application of the gate voltage. Because the gate-induced electric field in the QW opposes the initial electric field due to modulation doping on the bottom side of the QW, the increase of the hole concentration in the QW decreases its internal electric field. Thus, $\alpha_3 E_z$ decreases with increasing hole concentration.

Equation (1) suggests another interesting aspect of the cubic-Rashba coefficient. The Rashba coefficient can be strongly tuned with the HH-LH separation. We estimated α_3 using Eq. (1) with $\gamma_3 = 5.69$ for Ge [1]. The HH-LH separation for compressively strained-Ge/Si$_{0.5}$Ge$_{0.5}$ is $\sim$110 meV [31]. We obtained $\alpha_3 = 2.26 \times 10^5\ e\,$Å^4. The coefficient α_3 is about 1 order smaller than for the 2DHG in the GaAs/AlGaAs single heterostructure [21], which is a nearly lattice matched system. The smaller α_3 value is due to the large HH-LH separation in Ge/Si$_{0.5}$Ge$_{0.5}$ compared to that of the GaAs/AlGaAs structure; the large HH-LH separation decreases the coefficient α_3. In the strained-Ge/SiGe QW, the HH-LH separation can be tuned by the strain due to the SiGe layer; in other words, the composition x of the Si$_{1-x}$Ge$_x$ buffer layer enables a wide range of tuning options for the cubic-Rashba SOI. Note that Ge has a larger γ_3 value than Si ($\gamma_3 = 1.45$) [1]; thus we expect a larger SOI for the 2DHG in Ge than that of Si. Therefore strained Ge is a promising material for utilizing the cubic-Rashba SOI in a low dimensional system.

[*] moriyar@iis.u-tokyo.ac.jp
[†] tmachida@iis.u-tokyo.ac.jp
[‡] Present address: Graduate School of Engineering, Nagoya University, Nagoya 464-8603, Japan.
[1] R. Winkler, *Spin-Orbit Coupling Effects in Two-Dimensional Electron and Hole Systems* (Springer Berlin Heidelberg, 2003).
[2] T. Koga, J. Nitta, and M. van Veenhuizen, Phys. Rev. B **70**, 161302 (2004).
[3] T. Koga, Y. Sekine, and J. Nitta, Phys. Rev. B **74**, 041302 (2006).
[4] B. A. Bernevig, J. Orenstein, and S.-C. Zhang, Phys. Rev. Lett. **97**, 236601 (2006).
[5] J. D. Koralek, C. P. Weber, J. Orenstein, B. A. Bernevig, S.-C. Zhang, S. Mack, and D. D. Awschalom, Nature (London) **458**, 610 (2009).
[6] J. E. Hirsch, Phys. Rev. Lett. **83**, 1834 (1999).
[7] S. Murakami, N. Nagaosa, and S.-C. Zhang, Science **301**, 1348 (2003).
[8] Y. K. Kato, R. C. Myers, A. C. Gossard, and D. D. Awschalom, Science **306**, 1910 (2004).
[9] C. L. Kane and E. J. Mele, Phys. Rev. Lett. **95**, 146802 (2005).
[10] B. A. Bernevig and S.-C. Zhang, Phys. Rev. Lett. **96**, 106802 (2006).
[11] G. Dresselhaus, Phys. Rev. **100**, 580 (1955).
[12] E. I. Rashba, Sov. Phys. Solid State **2**, 1109 (1960).
[13] F. J. Ohkawa and Y. Uemura, J. Phys. Soc. Jpn. **37**, 1325 (1974).
[14] R. Winkler, D. Culcer, S. J. Papadakis, B. Habib, and M. Shayegan, Semicond. Sci. Technol. **23**, 114017 (2008).
[15] H. Nakamura, T. Koga, and T. Kimura, Phys. Rev. Lett. **108**, 206601 (2012).
[16] L. G. Gerchikov and A. V. Subashiev, Sov. Phys. Semicond. **26**, 73 (1992).
[17] J. Schliemann and D. Loss, Phys. Rev. B **71**, 085308 (2005).
[18] O. Bleibaum and S. Wachsmuth, Phys. Rev. B **74**, 195330 (2006).
[19] T. Ma and Q. Liu, Phys. Rev. B **73**, 245315 (2006).
[20] G. M. Minkov, A. A. Sherstobitov, A. V. Germanenko, O. E. Rut, V. A. Larionova, and B. N. Zvonkov, Phys. Rev. B **71**, 165312 (2005).
[21] R. Winkler, H. Noh, E. Tutuc, and M. Shayegan, Phys. Rev. B **65**, 155303 (2002).
[22] J. P. Lu, J. B. Yau, S. P. Shukla, M. Shayegan, L. Wissinger, U. Rössler, and R. Winkler, Phys. Rev. Lett. **81**, 1282 (1998).
[23] A. Dobbie, M. Myronov, R. J. H. Morris, A. H. A. Hassan, M. J. Prest, V. A. Shah, E. H. C. Parker, T. E. Whall, and D. R. Leadley, Appl. Phys. Lett. **101**, 172108 (2012).
[24] K. Sawano, K. Toyama, R. Masutomi, T. Okamoto, N. Usami, K. Arimoto, K. Nakagawa, and Y. Shiraki, Appl. Phys. Lett. **95**, 122109 (2009).
[25] T. Irisawa, M. Myronov, O. A. Mironov, E. H. C. Parker, K. Nakagawa, M. Murata, S. Koh, and Y. Shiraki, Appl. Phys. Lett. **82**, 1425 (2003).
[26] B. Rößner, G. Isella, and H. v. Känel, Appl. Phys. Lett. **82**, 754 (2003).
[27] S. V. Iordanskii, Y. B. Lyanda-Geller, and G. E. Pikus, JETP Lett. **60**, 206 (1994).
[28] See Supplemental Material at http://link.aps.org/supplemental/10.1103/PhysRevLett.113.086601 for details of the ILP theory used for fitting.
[29] I. Žutić, J. Fabian, and S. Das Sarma, Rev. Mod. Phys. **76**, 323 (2004).
[30] B. Habib, E. Tutuc, S. Melinte, M. Shayegan, D. Wasserman, S. A. Lyon, and R. Winkler, Appl. Phys. Lett. **85**, 3151 (2004).
[31] M. V. Fischetti and S. E. Laux, J. Appl. Phys. **80**, 2234 (1996).